Stem Cell Reports
Resource
OPEN ACCESS

Scarless Genome Editing of Human Pluripotent Stem Cells via Transient Puromycin Selection

Benjamin Steyer,[1,8] Qian Bu,[2,8] Evan Cory,[1] Keer Jiang,[2] Stella Duong,[2] Divya Sinha,[2,3] Stephanie Steltzer,[1] David Gamm,[2,3,4] Qiang Chang,[2,5,6,*] and Krishanu Saha[1,2,7,*]

[1]Wisconsin Institute for Discovery, University of Wisconsin-Madison, Madison, WI 53715, USA
[2]Waisman Center, University of Wisconsin-Madison, Madison, WI 53705, USA
[3]McPherson Eye Research Institute, University of Wisconsin-Madison, Madison, WI 53705, USA
[4]Department of Ophthalmology & Visual Sciences, University of Wisconsin-Madison, Madison, WI 53705, USA
[5]Department of Medical Genetics, University of Wisconsin School of Medicine and Public Health, Madison, WI 53705, USA
[6]Department of Neurology, University of Wisconsin School of Medicine and Public Health, Madison, WI 53705, USA
[7]Department of Biomedical Engineering, University of Wisconsin-Madison, Madison, WI 53706, USA
[8]Co-first author
*Correspondence: qchang@waisman.wisc.edu (Q.C.), ksaha@wisc.edu (K.S.)
https://doi.org/10.1016/j.stemcr.2017.12.004

SUMMARY

Genome-edited human pluripotent stem cells (hPSCs) have broad applications in disease modeling, drug discovery, and regenerative medicine. We present and characterize a robust method for rapid, scarless introduction or correction of disease-associated variants in hPSCs using CRISPR/Cas9. Utilizing non-integrated plasmid vectors that express a puromycin N-acetyl-transferase (PAC) gene, whose expression and translation is linked to that of Cas9, we transiently select for cells based on their early levels of Cas9 protein. Under optimized conditions, co-delivery with single-stranded donor DNA enabled isolation of clonal cell populations containing both heterozygous and homozygous precise genome edits in as little as 2 weeks without requiring cell sorting or high-throughput sequencing. Edited cells isolated using this method did not contain any detectable off-target mutations and displayed expected functional phenotypes after directed differentiation. We apply the approach to a variety of genomic loci in five hPSC lines cultured using both feeder and feeder-free conditions.

INTRODUCTION

Induced pluripotent stem cells (iPSCs) have had a profound impact on disease modeling, personalized drug screening, and autologous tissue replacement fields (Saha and Jaenisch, 2009). Genome editing technologies can further augment these important human pluripotent stem cell (hPSC) resources. CRISPR constitutes a key genome editing tool because of its robust performance in many cell and tissue types. The CRISPR/Cas9 system utilizes an endonuclease, Cas9, and a single-guide RNA (sgRNA) that complexes with Cas9 to produce targeted double-strand breaks (DSBs) in genomic DNA (Cong et al., 2013; Mali et al., 2013). DSBs are repaired primarily via two canonical DNA repair pathways: non-homologous end-joining (NHEJ), which often results in insertion and deletion (indel) mutations, and homology-directed repair (HDR). HDR utilizes template DNA (usually the homologous chromosome) to repair DNA in a precise or "error-free" manner. Delivering donor DNA, along with the CRISPR/Cas9 system, can co-opt the cell's intrinsic HDR machinery to integrate precise nucleotide changes, or edits, encoded by the donor.

HDR-mediated genome editing can be used to introduce or correct specific disease-associated variants for disease modeling. Unfortunately, the efficiency of HDR is low (<10%) in hPSCs, so initial efforts relied on integrated drug selection cassettes (delivered via plasmid or linear double-stranded DNA [dsDNA] donors) to efficiently identify edited clones (Lombardo et al., 2007). However, use of selection cassettes generally results in permanent integration of at least a portion of the cassette sequence. Integration of exogenous sequences may have unintended effects. For example, exogenous DNA sequences within splice sites, introns, and 5′ and 3′ non-coding regions can impact mRNA processing and/or protein translation (Zhao et al., 2017; Zhu et al., 2015). Thus, for precision disease-modeling applications, manipulation of only the desired sequence—without introduction of additional exogenous DNA or permanent integration of selection cassettes (herein referred to as "scarless editing")—is desired.

Scarless genome editing enables the creation of isogenic pairs of hPSCs, which differ only at the engineered point mutation. Isogenic pairs of hPSCs have provided key insights into the function of coding and non-coding variants for various diseases (Jacob et al., 2017; Soldner et al., 2016). Correction or introduction of disease-associated gene variants 1–20 nt in size has recently been accomplished through the use of short single-stranded oligonucleotide donors (ssODNs) with homology arms of 30–100 nt (Richardson et al., 2016; Yang et al., 2013). An advantage of ssODNs is that they can be synthesized rapidly, thus reducing labor and increasing throughput. Further, single-stranded DNA is less likely to randomly integrate into

the genome compared with plasmids or linear dsDNA donors (Li et al., 2017). The ssODN strategy results in scarless editing, but the lack of selectable markers encoded within the donor increases the difficulty of identifying precisely edited clones.

To increase generation and isolation of scarless gene-edited hPSCs, a substantial body of work (summarized in Table S1) has focused on several strategies: (1) increasing the efficiency of screening for edited clones, (2) increasing the ratio of HDR to NHEJ, and (3) improving overall (NHEJ and HDR) editing efficiency. First, identification of rare precisely genome-edited clones from a mixed population has been improved through the development of high-throughput genotyping methods (Miyaoka et al., 2014; Ramlee et al., 2015). These methods necessitate working with a high number of clonal cell lines (typically over a hundred) and can require specialized equipment. Recent PiggyBac transposon methods (Arias-Fuenzalida et al., 2017; Eggenschwiler et al., 2016) enable complete removal of selectable markers for scarless editing of hPSCs. These methods employ an additional step involving excision of the selectable marker from the edited clones. The requirement for temporary introduction of selection cassettes also transiently disrupts endogenous gene expression, which prevents their use in essential genes or those required for hPSC maintenance.

Second, improving HDR to NHEJ ratio has been accomplished through manipulation of intrinsic DSB repair processes. Controlled timing of Cas9 delivery in pro-HDR phases of the cell cycle was shown to increase HDR efficiency; however, the parameters for optimal HDR efficiency varied considerably from cell line to cell line (Lin et al., 2014). Another approach enriches for cells that are biased toward HDR through co-insertion of a selectable marker at a secondary safe-harbor locus (Mitzelfelt et al., 2017; Shy et al., 2016). Co-insertion methods address concerns regarding cell line to cell line variability, but they require generation of DSBs at additional genomic loci and can result in permanent integration of the selection cassette. Treatment of cells with factors that promote HDR or inhibit NHEJ (Chu et al., 2015; Maruyama et al., 2015; Song et al., 2016; Yu et al., 2015) and design improvements to the single-stranded donor DNA (Richardson et al., 2016) have also increased the occurrence of HDR in select genome editing experiments. However, the universal effectiveness of these approaches across many cell lines or at different genomic loci is still not clear (Song et al., 2016).

Third, efforts to improve overall editing efficiency indicate that Cas9 expression represents a universal limiting step in successful genome editing (Dow et al., 2015). Generating a parental cell line with inducible or constitutive Cas9 expression has been shown to yield NHEJ efficiencies of up to 60% and precise HDR efficiencies up to 40% (González et al., 2014; Liang et al., 2017). A limitation of these methods is that the Cas9 construct is either permanently integrated (González et al., 2014; Cao et al., 2016) or must be later removed with a subsequent reagent delivery and/or clonal selection step (Wang et al., 2017; Xie et al., 2017) to achieve scarless editing. Alternatively, non-integrating methods rely on enrichment of cells transiently expressing Cas9 through use of a selectable marker (Ding et al., 2013; Ran et al., 2013). Plasmids that utilize a viral 2A "ribosomal skip" peptide, to express GFP in stoichiometric proportion to Cas9, allow enrichment of Cas9 expressing cells based on fluorescence-assisted cell sorting (FACS). These methods have been generally adopted (Byrne and Church, 2015; Yang et al., 2013) and yield scarless HDR at efficiencies up to 6.0% in hPSCs. One limitation to these methods is the reliance on single-cell sorting to enrich for Cas9-expressing cells. Single-cell FACS can be challenging in hPSCs due to contamination risk and low survival: FACS methods must be optimized on a cell line to cell line basis to achieve 25% survival (Yang et al., 2013).

An alternative approach, focused on enriching for edited hPSCs without integration of selectable markers, employs co-transfection of a puromycin-resistance gene (puromycin N-acetyl-transferase [PAC]) along with standard CRISPR reagents (Horii et al., 2013). PAC expression can also be tied to Cas9 protein expression by utilizing the 2A ribosomal skipping approach (Ran et al., 2013). Previous work with this strategy has demonstrated utility in a handful of examples for gene knockout and scarless gene editing (Ran et al., 2013; Byrne et al., 2014). However, to our knowledge, there have been no reports on systematic optimization of this approach for scarless editing of multiple hPSC lines across different genomic loci.

Based on our previous work (Steyer et al., 2016), we hypothesized that stringent selection for cells expressing high levels of Cas9 might facilitate not only increased rates of gene knockout but also increased HDR when co-delivered with an ssODN. Puromycin is attractive for stringent transient selection as puromycin acts within days, and optimization requires only modifying the concentration and duration of puromycin treatment (Taniguchi et al., 1998). Below we test this strategy to edit four disease-relevant loci in five different cell lines and demonstrate the utility of this quick, effective, and low resource-intensive method for scarless gene editing of hPSCs.

RESULTS

Optimization of Transient Puromycin Selection in Pluripotent Cells

We sought to develop a simple, yet robust, workflow (Figure 1) to correct or introduce mutations in hPSCs without

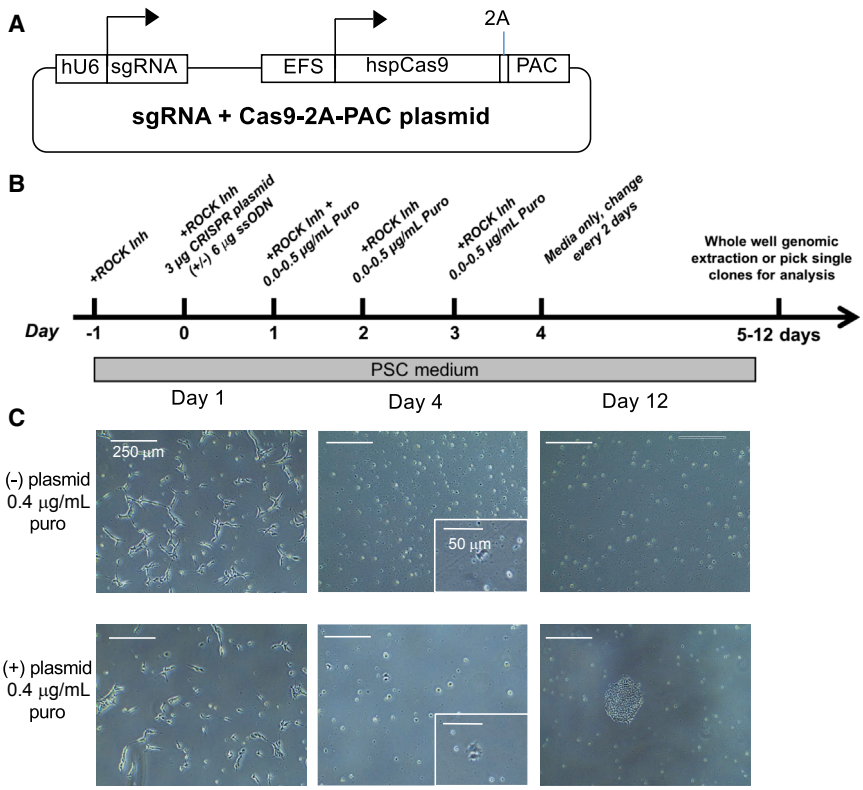

Figure 1. Transient Puromycin Selection Enriches for Precise HDR-Mediated Genome Editing in Pluripotent Stem Cells

(A) Schematic of sgRNA + Cas9-2A-PAC CRISPR plasmids. Expression of PAC is tied to human *Sp*Cas9 via a 2A peptide sequence. (B and C) Timeline and (C) representative images of transient puromycin selection. hPSCs were electroporated with sgRNA + Cas9-2A-PAC plasmid with or without ssODN, and were treated with puromycin from 24 to 96 hr (72 hr total) after electroporation. Minus (−) plasmid condition was electroporated under same conditions as experimental treatment, but without plasmid DNA.

FACS or extensive use of deep sequencing. Two previously described plasmids were selected that express both sgRNA and Cas9-2A-PAC (Ran et al., 2013; Sanjana et al., 2014) (Figure 1A). A single plasmid and ssODN design strategy for genome editing was used, as these reagents are widely available and less expensive to produce compared with mRNA or Cas9 protein reagents. We designed sgRNAs targeting specific heterozygous mutations in the *BEST1* gene within two unique patient-derived iPSC lines: BD6-4 (Figure S1A) and BD4-18 (Figure S1B). *BEST1* encodes a transmembrane ion channel expressed primarily in retinal pigment epithelium and specific mutations across the gene are associated with a group of individually distinct retinal dystrophies collectively termed bestrophinopathies (Guziewicz et al., 2017).

To start, plasmids encoding both Cas9-2A-PAC and a unique mutant (MT) allele targeting sgRNA were electroporated, without ssODN repair templates, into BD6-4 and BD4-18 iPSCs. Cells were seeded at a density of 15,000–20,000 cells/cm^2 and left to recover for 24 hr before 72-hr treatment with puromycin, ranging from 0.0 to 0.5 µg/mL, in medium supplemented with Rho kinase (ROCK) inhibitor (Figure 1B). By varying puromycin concentration we could identify conditions where iPSCs electroporated with sgRNA + Cas9-2A-PAC plasmid had visible clonal growth versus no survival in cells electroporated without Cas9-2A-PAC (Figure 1C). At 10–12 days post electroporation, we observed that, at some puromycin conditions (>0.3 µg/mL for BD6-4, >0.2 µg/mL for BD4-18), the surviving clones were mature enough for clonal picking but were still spatially separated (see representative image in Figure 1C). Notably, regarding cell line to cell line variation, BD6-4 cells transfected with Cas9-2A-PAC survived at 0.5 µg/mL puromycin treatment, while BD4-18 transfected cells did not survive selection at greater than 0.3 µg/mL puromycin (Figures S1A and S1B).

Genomic DNA was isolated from the cells that survived selection within each well and the targeted genomic region was deep sequenced after PCR amplification. Results indicate an increase in NHEJ editing as puromycin concentration increased (Figures S1A and S1B). Maximum editing was 24% at 0.5 µg/mL puromycin in BD6-4 and 25% at 0.3 µg/mL in BD4-18. The sgRNAs for each of these loci were designed to target only the heterozygous MT allele (Table S2), so in both cases the theoretical maximum NHEJ efficiency is 50%. To establish a recommended puromycin optimization range for other hPSCs, we repeated similar experiments in two putatively wild-type (WT) cell lines under feeder (irradiated mouse embryonic fibroblast [MEF]) and feeder-free (mTeSR1/Matrigel) culture conditions (Figure S1C). We observed that cells cultured on MEFs were more resistant to puromycin treatment than

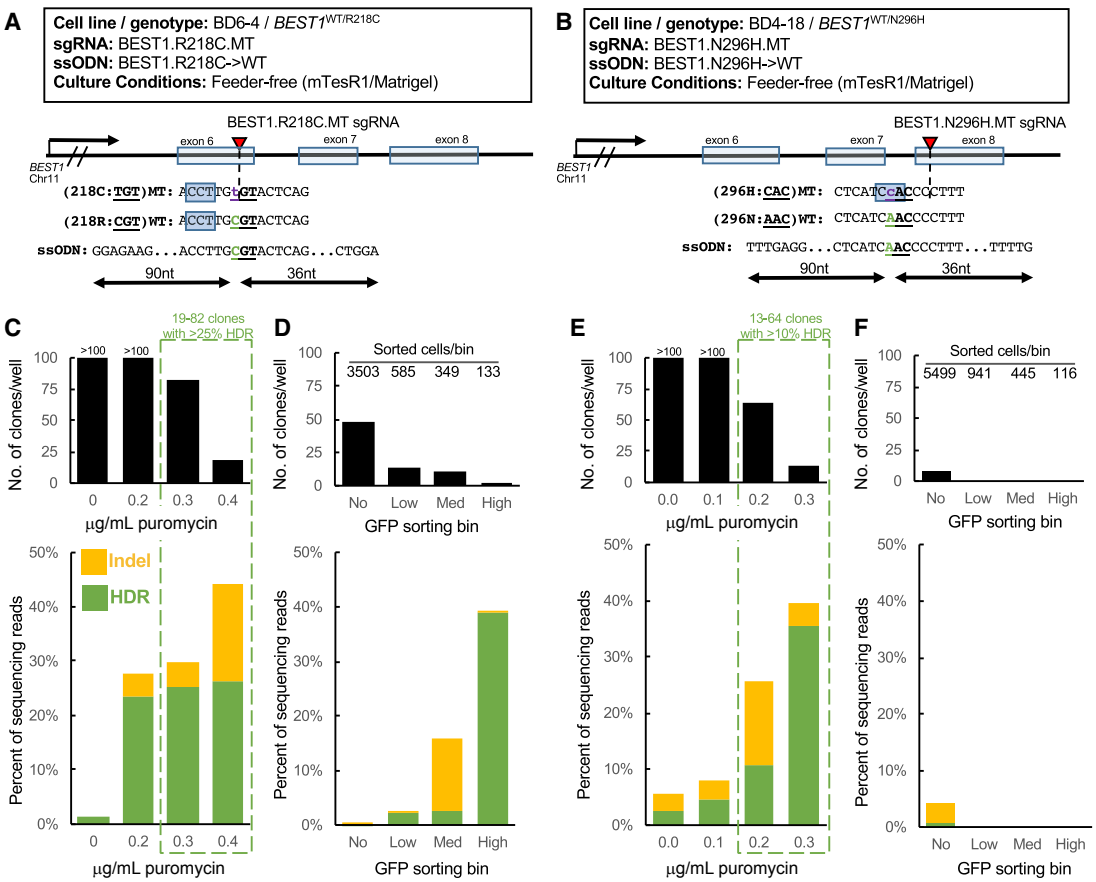

Figure 2. Comparison between Two Strategies of Selection after Delivery of CRISPR/Cas9 and ssODNs

(A) Genomic targeting for repair of heterozygous R218C mutation in BD6-4 line (genotype CGT/TGT) with repair ssODN. Red triangle indicates the predicted DSB cleavage site for the BEST1 R218C.MT sgRNA. Blue box denotes PAM site. Correction of MT allele to WT changes nucleotide (T > C) in the binding region of the sgRNA. On-target score for MT allele ~20-fold higher than score for WT allele (see Table S2).

(B) Genomic targeting for repair of heterozygous N296H mutation in BD4-18 line (genotype AAC/CAC) with repair ssODN. The red triangle indicates the target site for the BEST1 N296H.MT sgRNA. The blue box denotes PAM site. Correction of MT allele to WT sgRNA eliminates PAM site. On-target score for MT allele = 64.6. Off-target for WT allele was not ranked by scoring algorithm.

(C) Number of BD6-4 clones surviving puromycin selection and genome editing outcomes.

(D) Number of BD6-4 clones sorted into each GFP selection bin via FACS, number of clones surviving after 5- to 12-day recovery, and genome editing outcomes.

(E) Number of BD4-18 clones surviving puromycin selection and genome editing outcomes.

(F) Number of BD4-18 clones sorted into each GFP selection bin, number of clones surviving after 5- to 12-day recovery, and genome editing outcomes. No clones survived in GFP-positive BD4-18 populations. (E)–(H) each represent a single replicate. Genome editing outcomes determined by deep sequencing (see Data S1 in Supplement).

those cultured on Matrigel; however, a range of 0.2–0.5 µg/mL puromycin enabled the isolation of 20–200 clones per electroporation for all hPSC lines tested.

We next applied this method to test the efficiency of precise HDR-mediated genome editing in hPSCs (Figure 2). Cas9-2A-PAC plasmids also encoding the MT allele-specific sgRNA were delivered to both the BD-6-4 and BD4-18 cell line along with unique ssODNs designed to repair the MT allele to match the WT allele, without additional silent mutations (Figures 2A and 2B, bottom). The sgRNAs selected to cut near both the R218C and N296H mutations were predicted to have low or no affinity for the repaired WT genomic sequence (Table S2). Transient puromycin selection was performed over 72 hr at a range of puromycin concentrations shown previously to enrich for high NHEJ efficiency when edited without ssODN (Figure S1). At 12 days post electroporation, the number of distinct surviving clones was recorded (Figures 2C and 2E, top), and genomic DNA from cells within the entire well was extracted for locus-specific amplification and deep

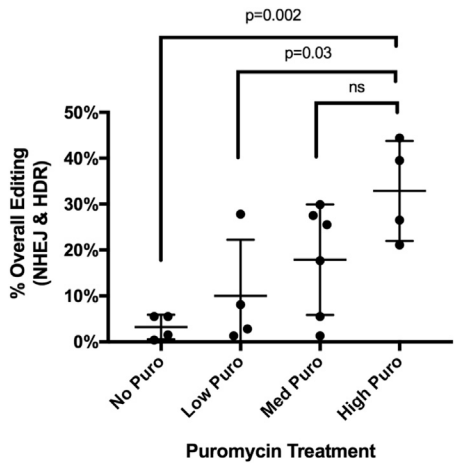

Figure 3. Overall Genome Editing Efficiency Increases with Increased Puromycin Selection Stringency

Plot includes overall editing (deep-sequencing read percentage) from unique puromycin-treatment conditions across Figures S1, 2C, and 2E (four electroporations). Med Puro (n = 6), all other conditions (n = 4). Error bars indicate ± SD of the mean. For description of puromycin condition groupings see Data S1 in Supplemental Information.

sequencing. The percentage of overall editing (NHEJ + HDR) increased up to approximately 40% over the range of puromycin concentrations tested for both BD6-4 and BD4-18 editing experiments (Figures 2C and 2E, bottom). Overall editing percentage increased as the number of clones surviving decreased, consistent with the results from conditions without ssODN (Figure S1). The percent of alleles undergoing precise HDR was greater than 25% at the highest puromycin concentration used for both experiments (Figures 2C and 2E, bottom). Selection conditions that generated approximately 20–80 clones per well (0.3–0.4 μg/mL for BD6-4 in Figure 2C and 0.2–0.3 μg/mL for BD4-18 in Figure 2E) had 10%–36% HDR with concomitant 3%–18% NHEJ, where HDR exceeded NHEJ for each condition. These results indicate that screening 24 surviving clones should identify 2–6 lines with repair of the heterozygous mutation and 2–4 lines with indel disruption of the MT allele.

We compared these results with an enrichment method that employs a plasmid encoding GFP in the place of PAC (Lonowski et al., 2017). To facilitate comparison, we electroporated both BD6-4 and BD4-18 lines with Cas9-2A-GFP + sgRNA plasmid and ssODN using identical transfection parameters to those used for PAC experiments. Cells were seeded in a single 10 cm^2 well for 24 hr to recover before FACS of the entire surviving population into four bins: No GFP, Low GFP, Medium GFP, and High GFP. The number of cells sorted and the number of surviving clones at 12 days after electroporation, for both cell lines, is shown in Figures 2D and 2F. Significantly lower cell survival was observed in the sorted GFP populations in comparison with puromycin-treatment conditions. In BD4-18 cells, only two clones survived sorting in the "No GFP" condition, and no clones were identified in any of the GFP-positive conditions. In BD6-4 cells, overall editing increased with GFP gate intensity. While around 40% of the reads in the "High GFP" were from alleles undergoing HDR, only two clones survived sorting (Figure 2F). In the "Low GFP" bin 14 clones survived and in the "Medium GFP" bin 11 clones survived, but little to no HDR was observed. There were no sorting conditions in these two cell lines that generated >15 clones per well with >10% HDR (Figures 2D and 2F). Collectively, results from BD6-4 and BD4-18 electroporations indicate that optimizing stringent selection with GFP expression to achieve high HDR—with an acceptable level of surviving clones—would require additional, possibly cell line-specific, optimization. Overall, population-based genome editing outcomes support the utility of stringent puromycin selection, indicating significant enrichment for edited cells as puromycin treatment is increased to medium- or high-selection conditions (Figure 3).

Clonal Analysis of Mutation-Corrected hPSCs

The utility of this method is dependent on isolation of precisely edited clones that are free of off-target edits and maintain their pluripotency and chromosomal stability. An advantage of stringent *in situ* puromycin selection is that 10–12 days post electroporation, unique hPSC clones are still spatially separated and can be individually picked for subcloning and Sanger sequencing. We repeated electroporations described in Figures 2A and 2B and results of correction of *BEST1* mutations are provided for both BD6-4 (Figure 4) and BD4-18 (Figure S2) lines. Transient puromycin selection at 0.4 μg/mL puromycin after electroporation of the heterozygous (WT/MT) BD6-4 line yielded 16 surviving clonal populations. Of these clones, seven displayed corrected, or WT/WT genotypes, five clones were unedited, or WT/MT, and four contained monoallelic indels or were non-clonal with indels (Figure 4B). These results are consistent with the population-based deep-sequencing data presented in Figure 2C.

A corrected clone isolated using this method was karyotypically normal (Figure 4C) and displayed pluripotency markers and tri-lineage differentiation potential (Figure 4D). Likewise, no indels were detected at the top five predicted off-target sites in the corrected clone when compared with the un-transfected parental line, an unedited clone, or clone with a mono-allelic indel isolated from the same electroporation (Figure S3A). Similar off-target analysis was performed for a corrected BD4-18 clone (Figure S2D). Importantly, the corrected BD6-4 clone remained puromycin sensitive after establishment of the cell line indicating that the puromycin-resistance cassette

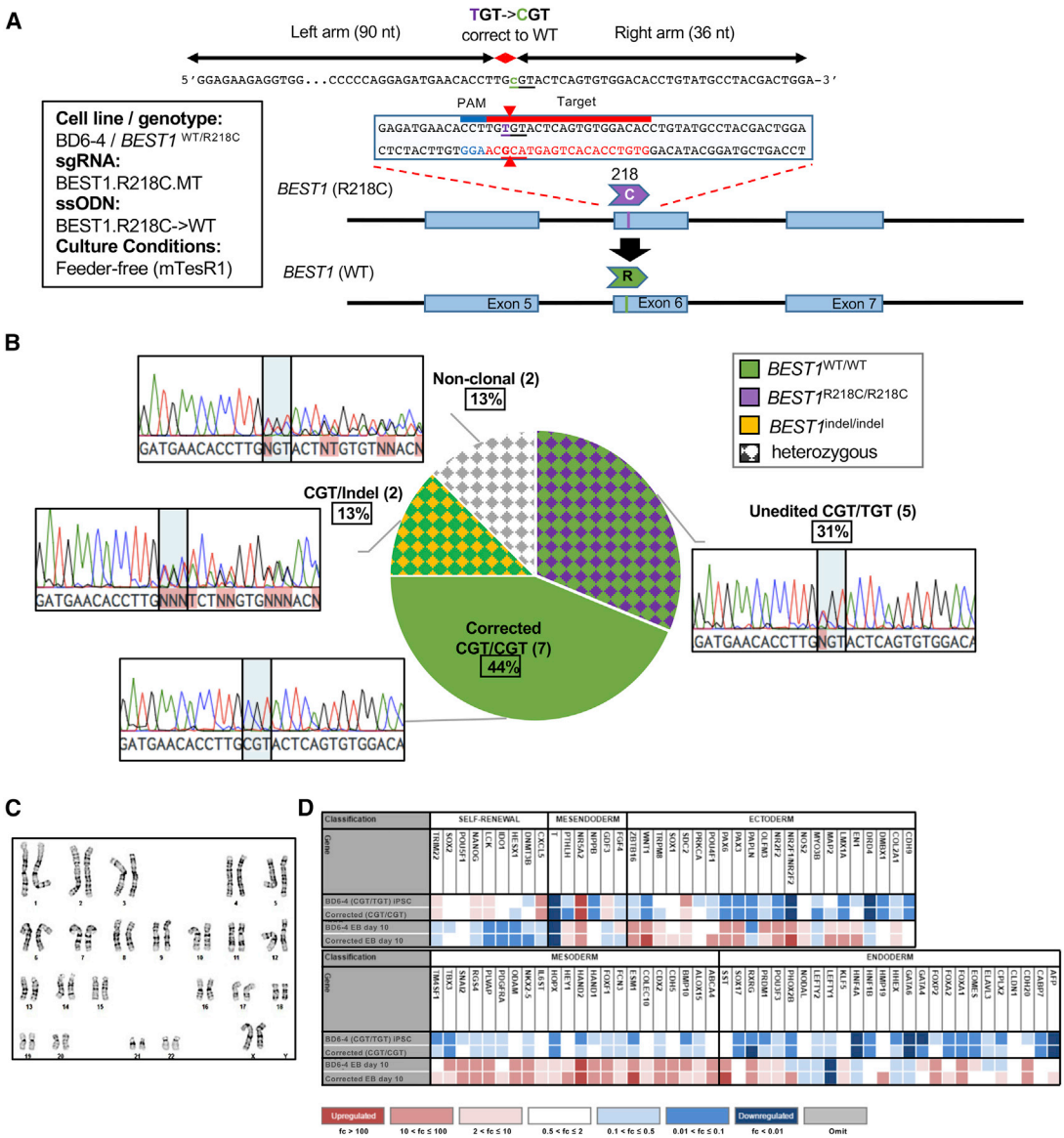

Figure 4. Precise Gene Correction of a Patient iPSC Line (BD6-4) Carrying a Heterozygous Mutation Using Transient Puromycin Selection

(A) Strategy for precision BEST1 R218C mutation correction. Top: sequence of ssODN used for scarless correction of point mutation in a single allele of the *BEST1* gene. Middle: PAM site is labeled in blue, the sgRNA target site is labeled in red, and red arrows indicate sgRNA DSB cleavage sites. Bottom: precise HDR-mediated editing causes correction of *BEST1*$^{WT/R218C}$ genotype to *BEST1*$^{WT/WT}$.

(B) Representative Sanger sequencing chromatograms of 16 clones surviving after puromycin selection from a single electroporation.

(C) Normal karyotype of selected gene corrected iPSC clone.

(D) TaqMan Scorecard (Thermo Fisher Scientific) gene expression panel indicating expression fold change (fc) of self-renewal, endoderm, ectoderm, and mesodermal markers for unedited (BD6-4) iPSCs, gene corrected iPSCs, and day 10 embryoid bodies derived from both cell lines compared with Scorecard reference database.

was not integrated (Figure S3B). Of note, a clone from a separate genome editing experiment designed to correct BD6-4 with a wobble codon for arginine was found to have an abnormal karyotype that is often associated with extended hPSC culture (Figure S4).

Mutation Introduction in Putatively WT hPSCs

Adapting the protocol described above, we next sought to perform scarless genome editing in putatively WT cell lines. We introduced precise disease-associated mutations (Figure 5) or synthetic stop cassettes (Figure S5) at endogenous

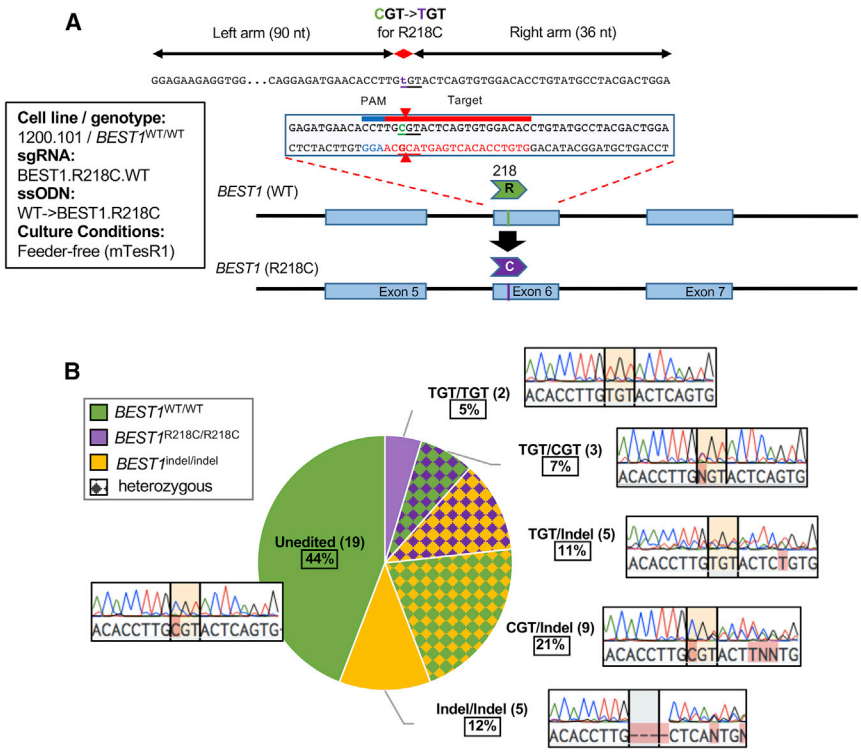

Figure 5. Efficient Isolation of Precise Heterozygous and Homozygous Genome-Edited Clones with Transient Puromycin Selection

(A) Strategy for precision BEST1 R218C mutation introduction. Top: sequence of ssODN used to introduce point mutation (i.e., knockin) into exon 6 of the *BEST1* gene. Middle: the PAM site is labeled in blue, the sgRNA target site is labeled in red, and red arrows indicate sgRNA DSB cleavage sites. Bottom: precise HDR-mediated editing causes c.1295C > T mutation to model disease-associated *BEST1*$^{WT/R218C}$ genotype (WT codon = CGT [Arg/R] MT codon = TGT [Cys/C]).

(B) Editing results broken down by diploid codon genotype for 43 randomly selected clones surviving transient puromycin selection from a single electroporation. Representative sequencing reads are displayed for each genotype. Electroporation and puromycin selection conditions are outlined in Figure S6.

loci on autosomal chromosomes. Such "engineering in" of disease-associated mutations into a putatively WT or normal cell line is desirable to create sets of isogenic cell lines for rigorous study of genotype-phenotype relationships (Hockemeyer and Jaenisch, 2016; Merkle and Eggan, 2013). First, we designed an sgRNA and ssODN to introduce a bestrophinopathy disease-associated mutation (R218C) in a WT (retinopathy free) iPSC line (1200.101) (Figure 5A). The mutation is within the target region of the sgRNA, so we made no changes to the ssODN, other than changing a single base to insert the mutation (Figure 5A, top sequence). DNA repair using this ssODN is predicted to introduce the R218C mutation in the *BEST1* locus (Figure 5A, bottom). This ssODN was electroporated along with the sgRNA + Cas9-2A-PAC plasmid, and cells were immediately plated in media supplemented with ROCK inhibitor with or without L755507 (Figure S6A). L755507 is a small molecule shown previously to increase HDR (Yu et al., 2015). After 24 hr of recovery, cells were exposed to transient puromycin selection at 0.5 μg/mL for 72 hr, based on the prior puromycin "kill curve" established for this cell line (data not shown). At 14 days, clonal populations were separated in culture and could be sampled for genomic extraction by picking only a portion of the colony while leaving the rest intact. The targeted locus of each clone was sequenced after PCR amplification. We observed little effect of L755507 treatment on genome editing outcomes (Figures S6B and S6C). Of the total of 43 clones picked and submitted to sequencing, 24 clones had editing (indel or HDR) at either one or both alleles (Figure 5B). The most common editing outcome was an indel in one allele (WT/indel, 9 out of 24) or both alleles (indel/indel, 5 out of 24). Three clones with heterozygous mutation introduction (WT/MT) and two clones with precise homozygous mutation introduction (MT/MT) were also observed. Desired clones were picked from the same population picked for genomic extraction and were transferred to a Matrigel-coated 24-well plate for expansion. Importantly, a single electroporation permitted the isolation of homozygous (MT/MT) clones with scarless introduction of the desired mutation, as well as heterozygous (WT/MT) clones without any indels or substitutions in the remaining WT allele. In a separate experiment in H9 hESCs, we were also able to isolate four clones with a desired stop cassette inserted into both chromodomain helicase DNA binding protein 8 (*CHD8*) alleles (MT/MT) by picking only 32 clones after transient puromycin selection (Figures S5B and S5C).

Homozygous X-Linked Mutation Insertion in hESCs

As an additional test of the robustness of this protocol, we designed an ssODN carrying R294X, and an sgRNA targeting the R294 position in the X-linked methyl-CpG binding protein 2 (*MECP2*) locus in H9 hESCs (Figure 6A).

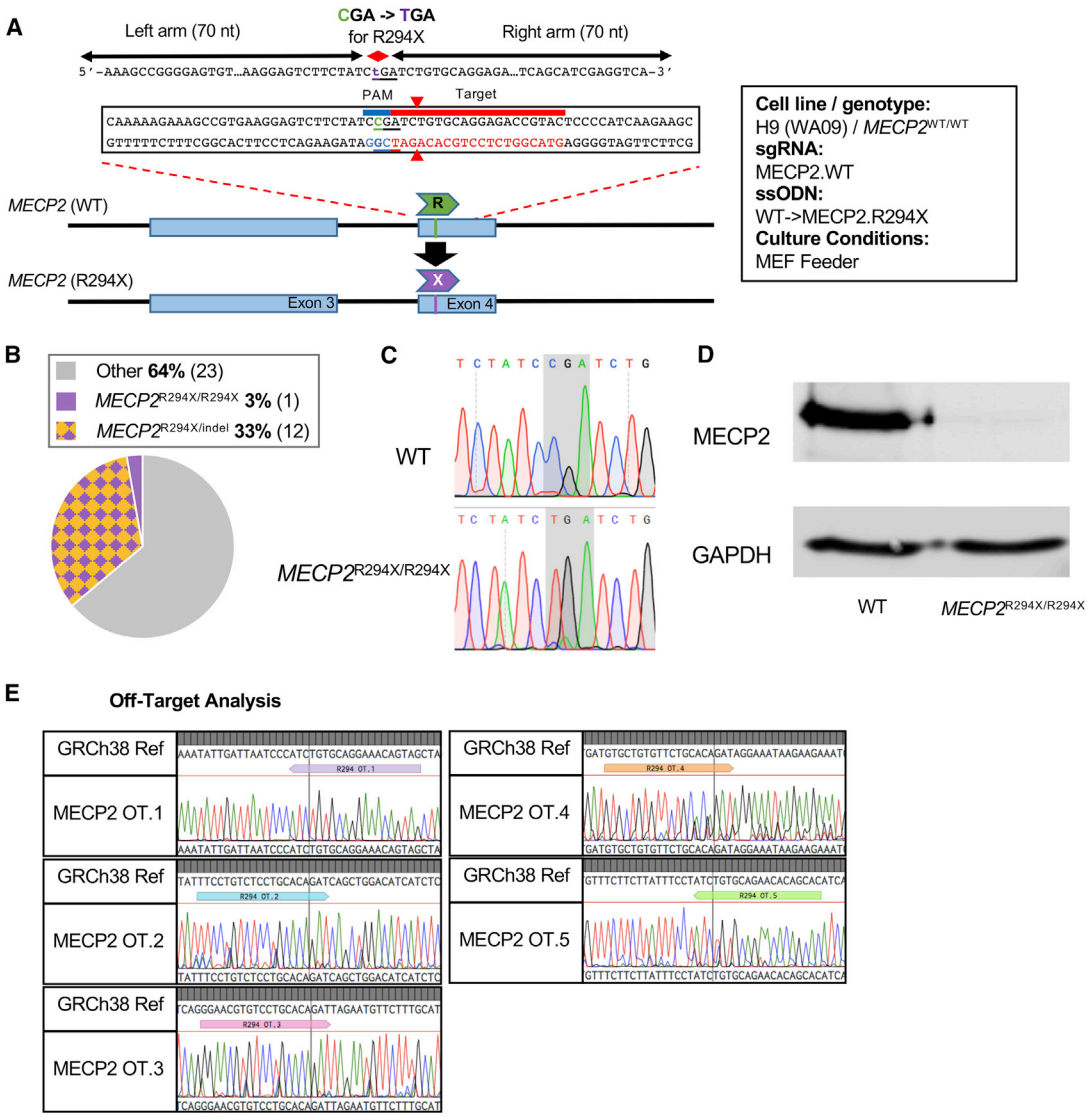

Figure 6. Isolation and Characterization of a Scarless Genome-Edited Clone Modified at the *MECP2* Locus on the X Chromosome

(A) Strategy for introducing an R294X mutation at the *MECP2* locus on the X chromosome in hESCs. Top: sequence of ssODN used to introduce point mutation into exon 4 of the *MECP2* gene. Middle: the PAM site is labeled in blue, the sgRNA target site is labeled in red, and red arrows indicate sgRNA DSB cleavage sites.

(B) The genotypes of 36 randomly selected clones from a single electroporation were analyzed by Sanger sequencing.

(C) Representative sequencing chromatograms of DNA from the parental H9 line and the *MECP2*$^{R294X/R294X}$ line. The WT codon (CGA) and stop codon (TGA) are shaded in gray.

(D) Western blot analyses of MECP2 protein level in H9 and *MECP2*$^{R294X/R294X}$ neuronal progenitors.

(E) Sequencing of top five predicted off-target sites for MECP2.WT sgRNA indicates no unintended introduction of indels in homozygous *MECP2*$^{R294X/R294X}$ clone.

Mutations of *MECP2* are associated with Rett syndrome, which is a debilitating developmental disorder (Amir et al., 1999). In female mammals, genes on one of the two X chromosomes undergo epigenetic silencing, a process referred to as X chromosome inactivation (XCI) (Lyon, 1999). The H9 hESC line is known to have a clonal XCI status, with a small percentage of reactivation of X-linked genes (Shen et al., 2008). The inactivated X chromosome condenses into a compact structure (Maxfield Boumil and Lee, 2001); therefore, it is expected that the Cas9-sgRNA complex will encounter difficulties in recognizing and binding to an inactive X chromosome locus to achieve homozygous editing (Kuscu et al., 2014; Singh et al., 2015; Wu et al., 2014). Using our approach, one

out of 36 clones was identified to be a homozygote for R294X, while 12 of 36 clones included R294X in one allele and indel in the other allele (Figure 6B). Sequencing of the WT and *MECP2*$^{R294X/R294X}$ hESC line verified that *MECP2*$^{R294X/R294X}$ hESC line contained a stop codon at the *MECP2* locus on both X chromosomes, including the inactive and presumably inaccessible X chromosome (Figure 6C). Western blot analysis revealed absence of full-length MECP2 protein in disease-relevant neuronal progenitor cells derived from the *MECP2*$^{R294X/R294X}$ hESC line (Figure 6D). Sanger sequencing was used to confirm the absence of off-target DSBs at the top five predicted off-target sites (Figure 6E).

DISCUSSION

The concept of transient puromycin selection for enrichment of cells with high Cas9 protein expression was proposed by Ran et al. (2013), however, we find that this method has not been widely applied to ssODN-mediated HDR in hPSCs. Our work demonstrates that, with minimal optimization, transient puromycin selection is a robust and efficient method for scarless HDR-mediated genome editing of hPSCs.

In comparison with other selection or enrichment methods, the workflow we describe here has some advantages. Integrated PAC expression from a plasmid donor is still employed for targeted insertion, but clones surviving selection frequently have random insertion of the resistance gene (Li et al., 2017; Zhu et al., 2015). Screening through surviving clones makes it inefficient to isolate precisely edited lines, which in some cases make up as few as 1 in 100 of colonies surviving puromycin selection (Soldner et al., 2011). Further, enrichment of cells expressing high levels of Cas9 via fluorescence (Li et al., 2014; Lonowski et al., 2017; Ran et al., 2013) or cell surface marker (Dever et al., 2016)-linked expression requires cell sorting, which requires cell line-specific optimization, and may lead to cell death in various hPSC lines (Lonowski et al., 2017; Ran et al., 2013; Wang et al., 2017). In our hands, we were unable to optimize the FACS procedure for one of our lines (Figure 2F). Transient puromycin selection must also be optimized for each cell line; however, this process is straightforward and, in our hands, required only a single puromycin "kill curve" to optimize selection stringency (Figures 1C and S1C). The main optimization constraint is to ensure rigorous selection for high Cas9 expression and translation in each cell line post delivery of the CRISPR components. Based on our observations, we suggest optimizing puromycin concentration in each new cell line to achieve post selection survival of 20–200 unique clones, from an initial electroporation of 1–2 million cells, to achieve the scarless editing rates presented here.

It is important to note that selecting for cells based on high expression of Cas9 has led to concerns over off-target effects, as several studies have shown that longer exposure or higher concentrations of active Cas9 can lead to a higher probability of off-target cutting (Chen et al., 2016; Kim et al., 2014). Off-target edits were likely minimized in this work by avoiding sgRNAs with low off-target scores (low score indicates more off-target cutting), as recommended by Hsu et al. (2013). However, a more comprehensive genome-wide analysis (Kim et al., 2015; Tsai et al., 2015) is required to definitively evaluate off-target editing.

Importantly, as with any stringent selection, puromycin treatment causes a population bottleneck that increases the possibility of selecting cell populations with non-specific growth or survival advantages. We encountered an abnormal karyotype in one of our hPSC clones isolated using the transient puromycin method (Figure S4). Pluripotent stem cells, in particular, are known to acquire common chromosomal translocations or point mutations over extended culture periods (Martins-Taylor and Xu, 2012; Merkle et al., 2017), and the specific genomic variant we observed is commonly associated with extended hPSC culture (Närvä et al., 2010). This limitation is shared by all protocols that employ clonal isolation (Hazelbaker et al., 2017), and may be an even greater concern in protocols that require more than one clonal selection step (Paquet et al., 2016; Shy et al., 2016). While we cannot definitively rule out other epigenetic or subkaryotypic genetic changes in all edited clones, we found that lines with normal karyotypes (400–500 band resolution) were pluripotent, differentiated properly, and displayed expected phenotypes.

A main advantage of the transient puromycin approach is the ability to rapidly optimize selection conditions for a variety of unique hPSC lines, increasingly collected in large stem cell banks and repositories (Turner et al., 2013). In contrast, methods that permanently (Cao et al., 2016; Dow et al., 2015; González et al., 2014) or reversibly (Wang et al., 2017; Xie et al., 2017) introduce Cas9 constructs to a cell line are advantageous when many edited cell lines will be generated from a single parental line. In addition, this workflow may facilitate efforts to interrogate disease-associated variants in rare or orphan diseases, where existing resource-intensive methodologies may not be not practical.

EXPERIMENTAL PROCEDURES

sgRNA Design Cas9 Vector Cloning

sgRNAs for each locus were selected using an online CRISPR design tool (crispr.mit.edu). All sgRNAs used for this work were 19 nucleotides in length upstream of an NGG PAM site. In general, sgRNAs were designed to overlap with the genomic mutation to prevent re-cutting of the genomic loci after mutation introduction or

correction. The mutation introduction or correction was designed to disrupt the PAM site, or to modify the genomic sequence as close to the "seed" region of the sgRNA (Pattanayak et al., 2013). On-target (Doench et al., 2016) and off-target (Hsu et al., 2013) scores greater than 40 (higher is better) were selected whenever possible to increase the performance and specificity of sgRNAs. All sgRNAs used for this study are listed in Table S2. Once selected, sgRNA sequences were ordered as primers from IDT (Iowa, USA) and amplified to form the sgRNA insert.

Plasmids designed for expression of sgRNA and Cas9-2A-PAC (62988 and 52961) or encoding sgRNA and Cas9-2A-GFP (48138) were obtained from Addgene. PCR-amplified sgRNA inserts (see Supplemental Experimental Procedures) were Gibson cloned (SGI) into the digested sgRNA + Cas9 plasmid and transformed into chemically competent *E. coli* (NEB). Clonal populations were sequenced to confirm integration of the intended sgRNA sequence. Confirmed plasmids were replicated, extracted, precipitated (using sodium acetate and ethanol) and resuspended in nuclease-free water.

Cell Lines

All work with human cell lines was carried out in accordance with institutional, national, and international guidelines and approved by the stem cell research oversight and biosafety committees at the University of Wisconsin-Madison.

Human iPSC cultures (BD6-4, BD4-18, 1013.202, and 1200.101) were reprogrammed from somatic cells by CDI (WI, USA) using episomal vectors. Human iPSC line BD4-18 was reprogrammed as described previously (Singh et al., 2013). Human ESC line H9 (passages 20–35) was obtained from WiCell Research Institute (WI, USA). For culture conditions see Supplemental Experimental Procedures.

Transfection and Transient Puromycin Selection

One day before electroporation, hPSCs were treated with ROCK inhibitor (10 μM Y-27632 [Selleck Chem] or 0.5 μM 555550 [Calbiochem]). At 60%–70% confluency, hPSCs were singularized with Accutase (Life Technologies) or TrypLE Express (Life Technologies). We utilized both a Gene Pulser Xcell (Bio-Rad) and an Amaxa 4D-Nucleofector (Lonza) for CRISPR/Cas9 delivery. For delivery using the Gene Pulser system, 2 million cells were electroporated with 15 μg of sgRNA plus Cas9-2A-PAC plasmid, with or without 30 μg of donor ssODN. The following settings were programmed into the Gene Pulser system: 250 V, 750 μF, infinity Ω; cuvette: 4 mm. For delivery using the 4D system, 800,000 cells were electroporated with 3 μg of sgRNA plus Cas9-2A-PAC plasmid and 6 μg of donor ssODN. The P3 Primary Cell kit with 100 μL cuvettes (Lonza) and program CA-137 was used as per the manufacturer's instructions. Post electroporation with either device, cells were plated at ~150,000 cells/well of 6-well plate (10 cm^2) and cultured per conditions outlined in Figure 1B. Starting 24 hr after electroporation, various concentrations of puromycin (Alfa Aesar) ranging from 0.0 to 0.7 μg/mL were added to the culture medium. After 3 days of puromycin selection, hPSCs were switched to their normal culture medium and fed every other day until ~1–2 weeks after electroporation when distinct colonies were established.

FACS

FACS of GFP-positive iPSCs 24 hr after electroporation was performed using a BD FACS Aria. One day before sorting, PSCs were treated with 10 μM Y-27632. Cells were singularized with TrypLE Express (Life Technologies). Voltages were established by running iPSCs transfected with pmaxGFP Control Vector (Lonza). Cells were sorted into four populations based on GFP intensity: No GFP, Low GFP, Med GFP, and High GFP. Each population was sorted into 4 mL of mTeSR +10 μM Y-27632 and plated into single well of a six-well plate (area ~10 cm^2).

Statistical Methods

Statistical analyses were performed using Prism 7 (GraphPad). Error bars indicate ± SD of the mean. Significance was determined by unpaired, two-tailed Student's t tests.

ACCESSION NUMBERS

The accession numbers for the deep-sequencing data reported in this paper are NCBI SRA: SRR6181595 and SRR6181596.

SUPPLEMENTAL INFORMATION

Supplemental Information includes Supplemental Experimental Procedures, six figures, four tables, and one data file and can be found with this article online at https://doi.org/10.1016/j.stemcr.2017.12.004.

AUTHOR CONTRIBUTIONS

B.S. and Q.B. planned the research. B.S., Q.B., D.S., Q.C., and K.S. helped design the experiments. B.S., Q.B., E.C., K.J., S.D., and S.S. performed experiments and analyzed the data. B.S., Q.B., and E.C. wrote the manuscript with input from all authors. D.G., Q.B., and K.S. supervised the research.

ACKNOWLEDGMENTS

This work was supported by the NSF (CBET-1350178 and CBET-1645123 to K.S.); the NIH (R35GM119644 to K.S., R03HD086523 to Q.C., R01EY024588 to D.G., T32HG002760 and F30EY027699 to B.S.); the VitreoRetinal Surgery Foundation to B.S.; Research to Prevent Blindness to D.G.; the Foundation Fighting Blindness to D.G.; the John Merck Fund (Translational Research Program to K.S.); the Brain & Behavior Research Foundation (to K.S.); and the Burroughs Wellcome Fund (to K.S.). This study was supported in part by a core grant to the Waisman Center from the National Institute of Child Health and Human Development (U54 HD090256). In addition, we thank all members of the Saha, Gamm, and Chang labs for comments on the manuscript. We also thank plasmid depositors to Addgene and the University of Wisconsin Biotechnology Center for DNA sequencing.

Received: April 14, 2017
Revised: December 1, 2017
Accepted: December 5, 2017
Published: January 4, 2018

REFERENCES

Amir, R.E., Van den Veyver, I.B., Wan, M., Tran, C.Q., Francke, U., and Zoghbi, H.Y. (1999). Rett syndrome is caused by mutations in X-linked MECP2, encoding methyl-CpG-binding protein 2. Nat. Genet. *23*, 185–188.

Arias-Fuenzalida, J., Jarazo, J., Qing, X., Walter, J., Gomez-Giro, G., Nickels, S.L., Zaehres, H., Schöler, H.R., and Schwamborn, J.C. (2017). FACS-assisted CRISPR-Cas9 genome editing facilitates Parkinson's disease modeling. Stem Cell Reports *9*, 1423–1431.

Byrne, S.M., and Church, G.M. (2015). CRISPR-mediated gene targeting of human induced pluripotent stem cells. Curr. Protoc. Stem Cell Biol. *35*, 1–22.

Byrne, S.M., Mali, P., and Church, G.M. (2014). Genome editing in human stem cells. Methods Enzymol. *546*, 119–138.

Cao, J., Wu, L., Zhang, S.-M., Lu, M., Cheung, W.K.C., Cai, W., Gale, M., Xu, Q., and Yan, Q. (2016). An easy and efficient inducible CRISPR/Cas9 platform with improved specificity for multiple gene targeting. Nucleic Acids Res. *44*, e149.

Chen, Y., Liu, X., Zhang, Y., Wang, H., Ying, H., Liu, M., Li, D., Lui, K.O., and Ding, Q. (2016). A self-restricted CRISPR system to reduce off-target effects. Mol. Ther. *24*, 1508–1510.

Chu, V.T., Weber, T., Wefers, B., Wurst, W., Sander, S., Rajewsky, K., and Kühn, R. (2015). Increasing the efficiency of homology-directed repair for CRISPR-Cas9-induced precise gene editing in mammalian cells. Nat. Biotechnol. *33*, 543–548.

Cong, L., Ran, F.A., Cox, D., Lin, S., Barretto, R., Habib, N., Hsu, P.D., Wu, X., Jiang, W., Marraffini, L.A., et al. (2013). Multiplex genome engineering using CRISPR/Cas systems. Science *339*, 819–823.

Dever, D.P., Bak, R.O., Reinisch, A., Camarena, J., Washington, G., Nicolas, C.E., Pavel-Dinu, M., Saxena, N., Wilkens, A.B., Mantri, S., et al. (2016). CRISPR/Cas9 β-globin gene targeting in human haematopoietic stem cells. Nature *539*, 384–389.

Ding, Q., Regan, S.N., Xia, Y., Oostrom, L.A., Cowan, C.A., and Musunuru, K. (2013). Enhanced efficiency of human pluripotent stem cell genome editing through replacing TALENs with CRISPRs. Cell Stem Cell *12*, 393–394.

Doench, J.G., Fusi, N., Sullender, M., Hegde, M., Vaimberg, E.W., Donovan, K.F., Smith, I., Tothova, Z., Wilen, C., Orchard, R., et al. (2016). Optimized sgRNA design to maximize activity and minimize off-target effects of CRISPR-Cas9. Nat. Biotechnol. *34*, 184–191.

Dow, L.E., Fisher, J., O'Rourke, K.P., Muley, A., Kastenhuber, E.R., Livshits, G., Tschaharganeh, D.F., Socci, N.D., and Lowe, S.W. (2015). Inducible in vivo genome editing with CRISPR-Cas9. Nat. Biotechnol. *33*, 390–394.

Eggenschwiler, R., Moslem, M., Fráguas, M.S., Galla, M., Papp, O., Naujock, M., Fonfara, I., Gensch, I., Wähner, A., Beh-Pajooh, A., et al. (2016). Improved bi-allelic modification of a transcriptionally silent locus in patient-derived iPSC by Cas9 nickase. Sci. Rep. *6*, 38198.

González, F., Zhu, Z., Shi, Z.-D., Lelli, K., Verma, N., Li, Q.V., and Huangfu, D. (2014). An iCRISPR platform for rapid, multiplexable, and inducible genome editing in human pluripotent stem cells. Cell Stem Cell *15*, 215–226.

Guziewicz, K.E., Sinha, D., Gómez, N.M., Zorych, K., Dutrow, E.V., Dhingra, A., Mullins, R.F., Stone, E.M., Gamm, D.M., Boesze-Battaglia, K., et al. (2017). Bestrophinopathy: an RPE-photoreceptor interface disease. Prog. Retin. Eye Res. *58*, 70–88.

Hazelbaker, D.Z., Beccard, A., Bara, A.M., Dabkowski, N., Messana, A., Mazzucato, P., Lam, D., Manning, D., Eggan, K., and Barrett, L.E. (2017). A scaled framework for CRISPR editing of human pluripotent stem cells to study psychiatric disease. Stem Cell Reports *9*, 1315–1327.

Hockemeyer, D., and Jaenisch, R. (2016). Induced pluripotent stem cells meet genome editing. Cell Stem Cell *18*, 573–586.

Horii, T., Morita, S., Kimura, M., Kobayashi, R., Tamura, D., Takahashi, R., Kimura, H., Suetake, I., Ohata, H., Okamoto, K., et al. (2013). Genome engineering of mammalian haploid embryonic stem cells using the Cas9/RNA system. PeerJ *1*, e230.

Hsu, P.D., Scott, D.A., Weinstein, J.A., Ran, F.A., Konermann, S., Agarwala, V., Li, Y., Fine, E.J., Wu, X., Shalem, O., et al. (2013). DNA targeting specificity of RNA-guided Cas9 nucleases. Nat. Biotechnol. *31*, 827–832.

Jacob, A., Morley, M., Hawkins, F., McCauley, K.B., Jean, J.C., Heins, H., Na, C.-L., Weaver, T.E., Vedaie, M., Hurley, K., et al. (2017). Differentiation of human pluripotent stem cells into functional lung alveolar epithelial cells. Cell Stem Cell *21*, 472–488.e10.

Kim, D., Bae, S., Park, J., Kim, E., Kim, S., Yu, H.R., Hwang, J., Kim, J.-I., and Kim, J.-S. (2015). Digenome-seq: genome-wide profiling of CRISPR-Cas9 off-target effects in human cells. Nat. Methods *12*, 237–243.

Kim, S., Kim, D., Cho, S.W., Kim, J., and Kim, J.-S. (2014). Highly efficient RNA-guided genome editing in human cells via delivery of purified Cas9 ribonucleoproteins. Genome Res. *24*, 1012–1019.

Kuscu, C., Arslan, S., Singh, R., Thorpe, J., and Adli, M. (2014). Genome-wide analysis reveals characteristics of off-target sites bound by the Cas9 endonuclease. Nat. Biotechnol. *32*, 677–683.

Li, H., Beckman, K.A., Pessino, V., Huang, B., Weissman, J.S., and Leonetti, M.D. (2017). Design and specificity of long ssDNA donors for CRISPR-based knock-in. bioRxiv. 178905.

Li, K., Wang, G., Andersen, T., Zhou, P., and Pu, W.T. (2014). Optimization of genome engineering approaches with the CRISPR/Cas9 system. PLoS One *9*, e105779.

Liang, X., Potter, J., Kumar, S., Ravinder, N., and Chesnut, J.D. (2017). Enhanced CRISPR/Cas9-mediated precise genome editing by improved design and delivery of gRNA, Cas9 nuclease, and donor DNA. J. Biotechnol. *241*, 136–146.

Lin, S., Staahl, B.T., Alla, R.K., and Doudna, J.A. (2014). Enhanced homology-directed human genome engineering by controlled timing of CRISPR/Cas9 delivery. Elife *3*, e04766.

Lombardo, A., Genovese, P., Beausejour, C.M., Colleoni, S., Lee, Y.-L., Kim, K.A., Ando, D., Urnov, F.D., Galli, C., Gregory, P.D., et al. (2007). Gene editing in human stem cells using zinc finger nucleases and integrase-defective lentiviral vector delivery. Nat. Biotechnol. *25*, 1298–1306.

Lonowski, L.A., Narimatsu, Y., Riaz, A., Delay, C.E., Yang, Z., Niola, F., Duda, K., Ober, E.A., Clausen, H., Wandall, H.H., et al. (2017). Genome editing using FACS enrichment of nuclease-expressing cells and indel detection by amplicon analysis. Nat. Protoc. *12*, 581–603.

Lyon, M.F. (1999). X-Chromosome inactivation. Curr. Biol. *9*, R235–R237.

Mali, P., Yang, L., Esvelt, K.M., Aach, J., Guell, M., DiCarlo, J.E., Norville, J.E., and Church, G.M. (2013). RNA-guided human genome engineering via Cas9. Science *339*, 823–826.

Martins-Taylor, K., and Xu, R.H. (2012). Concise review: genomic stability of human induced pluripotent stem cells. Stem Cells *30*, 22–27.

Maruyama, T., Dougan, S.K., Truttmann, M.C., Bilate, A.M., Ingram, J.R., and Ploegh, H.L. (2015). Increasing the efficiency of precise genome editing with CRISPR-Cas9 by inhibition of nonhomologous end joining. Nat. Biotechnol. *33*, 538–542.

Maxfield Boumil, R., and Lee, J.T. (2001). Forty years of decoding the silence in X-chromosome inactivation. Hum. Mol. Genet. *10*, 2225–2232.

Merkle, F.T., and Eggan, K. (2013). Modeling human disease with pluripotent stem cells: from genome association to function. Cell Stem Cell *12*, 656–668.

Merkle, F.T., Ghosh, S., Kamitaki, N., Mitchell, J., Avior, Y., Mello, C., Kashin, S., Mekhoubad, S., Ilic, D., Charlton, M., et al. (2017). Human pluripotent stem cells recurrently acquire and expand dominant negative P53 mutations. Nature *545*, 229–233.

Mitzelfelt, K.A., McDermott-Roe, C., Grzybowski, M.N., Marquez, M., Kuo, C.-T., Riedel, M., Lai, S., Choi, M.J., Kolander, K.D., Helbling, D., et al. (2017). Efficient precision genome editing in iPSCs via genetic co-targeting with selection. Stem Cell Reports *8*, 491–499.

Miyaoka, Y., Chan, A.H., Judge, L.M., Yoo, J., Huang, M., Nguyen, T.D., Lizarraga, P.P., So, P.-L., and Conklin, B.R. (2014). Isolation of single-base genome-edited human iPS cells without antibiotic selection. Nat. Methods *11*, 291–293.

Närvä, E., Autio, R., Rahkonen, N., Kong, L., Harrison, N., Kitsberg, D., Borghese, L., Itskovitz-Eldor, J., Rasool, O., Dvorak, P., et al. (2010). High-resolution DNA analysis of human embryonic stem cell lines reveals culture-induced copy number changes and loss of heterozygosity. Nat. Biotechnol. *28*, 371–377.

Paquet, D., Kwart, D., Chen, A., Sproul, A., Jacob, S., Teo, S., Olsen, K.M., Gregg, A., Noggle, S., and Tessier-Lavigne, M. (2016). Efficient introduction of specific homozygous and heterozygous mutations using CRISPR/Cas9. Nature *533*, 125–129.

Pattanayak, V., Lin, S., Guilinger, J.P., Ma, E., Doudna, J.A., and Liu, D.R. (2013). High-throughput profiling of off-target DNA cleavage reveals RNA-programmed Cas9 nuclease specificity. Nat. Biotechnol. *31*, 839–843.

Ramlee, M.K., Yan, T., Cheung, A.M.S., Chuah, C.T.H., and Li, S. (2015). High-throughput genotyping of CRISPR/Cas9-mediated mutants using fluorescent PCR-capillary gel electrophoresis. Sci. Rep. *5*, 15587.

Ran, F.A., Hsu, P.D., Wright, J., Agarwala, V., Scott, D.A., and Zhang, F. (2013). Genome engineering using the CRISPR-Cas9 system. Nat. Protoc. *8*, 2281–2308.

Richardson, C.D., Ray, G.J., DeWitt, M.A., Curie, G.L., and Corn, J.E. (2016). Enhancing homology-directed genome editing by catalytically active and inactive CRISPR-Cas9 using asymmetric donor DNA. Nat. Biotechnol. *34*, 339–344.

Saha, K., and Jaenisch, R. (2009). Technical challenges in using human induced pluripotent stem cells to model disease. Cell Stem Cell *5*, 584–595.

Sanjana, N.E., Shalem, O., and Zhang, F. (2014). Improved vectors and genome-wide libraries for CRISPR screening. Nat. Methods *11*, 783–784.

Shen, Y., Matsuno, Y., Fouse, S.D., Rao, N., Root, S., Xu, R., Pellegrini, M., Riggs, A.D., and Fan, G. (2008). X-Inactivation in female human embryonic stem cells is in a nonrandom pattern and prone to epigenetic alterations. Proc. Natl. Acad. Sci. USA *105*, 4709–4714.

Shy, B.R., MacDougall, M.S., Clarke, R., and Merrill, B.J. (2016). Co-incident insertion enables high efficiency genome engineering in mouse embryonic stem cells. Nucleic Acids Res. *44*, 7997–8010.

Singh, R., Shen, W., Kuai, D., Martin, J.M., Guo, X., Smith, M.A., Perez, E.T., Phillips, M.J., Simonett, J.M., Wallace, K.A., et al. (2013). iPS cell modeling of Best disease: insights into the pathophysiology of an inherited macular degeneration. Hum. Mol. Genet. *22*, 593–607.

Singh, R., Kuscu, C., Quinlan, A., Qi, Y., and Adli, M. (2015). Cas9-chromatin binding information enables more accurate CRISPR off-target prediction. Nucleic Acids Res. *43*, e118.

Soldner, F., Laganière, J., Cheng, A.W., Hockemeyer, D., Gao, Q., Alagappan, R., Khurana, V., Golbe, L.I., Myers, R.H., Lindquist, S., et al. (2011). Generation of isogenic pluripotent stem cells differing exclusively at two early onset Parkinson point mutations. Cell *146*, 318–331.

Soldner, F., Stelzer, Y., Shivalila, C.S., Abraham, B.J., Latourelle, J.C., Barrasa, M.I., Goldmann, J., Myers, R.H., Young, R.A., and Jaenisch, R. (2016). Parkinson-associated risk variant in distal enhancer of α-synuclein modulates target gene expression. Nature *533*, 95–99.

Song, J., Yang, D., Xu, J., Zhu, T., Chen, Y.E., and Zhang, J. (2016). RS-1 enhances CRISPR/Cas9- and TALEN-mediated knock-in efficiency. Nat. Commun. *7*, 10548.

Steyer, B., Carlson-Stevermer, J., Angenent-Mari, N., Khalil, A., Harkness, T., and Saha, K. (2016). High content analysis platform for optimization of lipid mediated CRISPR-Cas9 delivery strategies in human cells. Acta Biomater. *34*, 143–158.

Taniguchi, M., Sanbo, M., Watanabe, S., Naruse, I., Mishina, M., and Yagi, T. (1998). Efficient production of Cre-mediated site-directed recombinants through the utilization of the puromycin resistance gene, pac: a transient gene-integration marker for ES cells. Nucleic Acids Res. *26*, 679–680.

Tsai, S.Q., Zheng, Z., Nguyen, N.T., Liebers, M., Topkar, V.V., Thapar, V., Wyvekens, N., Khayter, C., Iafrate, A.J., Le, L.P., et al. (2015). GUIDE-seq enables genome-wide profiling of off-target cleavage by CRISPR-Cas nucleases. Nat. Biotechnol. *33*, 187–197.

Turner, M., Leslie, S., Martin, N.G., Peschanski, M., Rao, M., Taylor, C.J., Trounson, A., Turner, D., Yamanaka, S., and Wilmut, I. (2013). Toward the development of a global induced pluripotent stem cell library. Cell Stem Cell *13*, 382–384.

Wang, G., Yang, L., Grishin, D., Rios, X., Ye, L.Y., Hu, Y., Li, K., Zhang, D., Church, G.M., and Pu, W.T. (2017). Efficient, footprint-free human iPSC genome editing by consolidation of Cas9/CRISPR and piggyBac technologies. Nat. Protoc. *12*, 88–103.

Wu, X., Scott, D.A., Kriz, A.J., Chiu, A.C., Hsu, P.D., Dadon, D.B., Cheng, A.W., Trevino, A.E., Konermann, S., Chen, S., et al. (2014). Genome-wide binding of the CRISPR endonuclease Cas9 in mammalian cells. Nat. Biotechnol. *32*, 670–676.

Xie, Y., Wang, D., Lan, F., Wei, G., Ni, T., Chai, R., Liu, D., Hu, S., Li, M., Li, D., et al. (2017). An episomal vector-based CRISPR/Cas9 system for highly efficient gene knockout in human pluripotent stem cells. Sci. Rep. *7*, 2320.

Yang, L., Guell, M., Byrne, S., Yang, J.L., Angeles, A.D.L., Mali, P., Aach, J., Kim-Kiselak, C., Briggs, A.W., Rios, X., et al. (2013). Optimization of scarless human stem cell genome editing. Nucleic Acids Res. *41*, 9049–9061.

Yu, C., Liu, Y., Ma, T., Liu, K., Xu, S., Zhang, Y., Liu, H., La Russa, M., Xie, M., Ding, S., et al. (2015). Small molecules enhance CRISPR genome editing in pluripotent stem cells. Cell Stem Cell *16*, 142–147.

Zhao, W., Siegel, D., Biton, A., Tonqueze, O.L., Zaitlen, N., Ahituv, N., and Erle, D.J. (2017). CRISPR-Cas9-mediated functional dissection of 3′-UTRs. Nucleic Acids Res. *45*, 10800–10810.

Zhu, Z., Verma, N., González, F., Shi, Z.D., and Huangfu, D. (2015). A CRISPR/Cas-mediated selection-free knockin strategy in human embryonic stem cells. Stem Cell Reports *4*, 1103–1111.